

# OPERATION AND ANALYSIS OF A NANOPOSITIONING AND NANOMEASURING MACHINE

Gerd Jäger, Eberhard Manske, Tino Hausotte and Walter Schott  
Technische Universität Ilmenau, Germany, 98684 Ilmenau, P.O. Box 100 565

**Key words:** nanomeasuring, nanopositioning, interferometers, nanometer-accuracy

## 1 Introduction

Nanopositioning and nanomeasuring machines (NPM machines) are technological means of positioning, measurement, scan, treatment and manipulation of objects with nanometer precision. Current and future high technologies such as microelectronics, micromechanics, optics, molecular biology and material engineering demand increasing ranges of motion, extreme precision and high positioning speeds. Furthermore, novel probe systems and nanotools have to be integrated into these machines to make them suitable for various tasks such as nanostructuring, mask and wafer inspection, large-area scanning probe microscopy, biotechnology and genetic engineering as well as measuring mechanical precision workpieces, precision treatment and assembly in the field of micro- and nanotechnology or for engineering new materials.

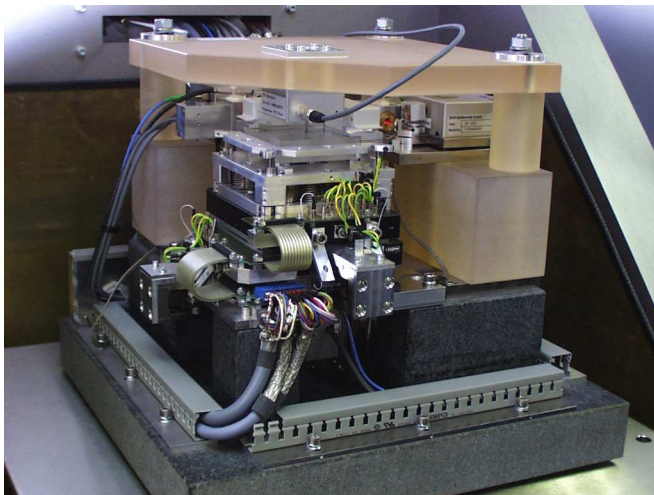


Figure 1: Nanopositioning and nanomeasuring machine with an optical probe system

At the Institute of Process Measurement and Sensor Technology of the *Technische Universität Ilmenau*, an NPM machine with the following parameters has been developed and successfully tested: positioning and measuring range 25 mm x 25 mm x 5 mm, resolution 1.24 nm and 0.1 nm, respectively, positioning uncertainty < 10 nm. The outstanding precision has been obtained by realizing the Abbe comparator principle in all three measuring axes and applying a new concept for compensating systematic errors resulting from mechanical guide systems. The machines have been manufactured by the *SIOS Messtechnik GmbH* company, Ilmenau. Up to now, three NPM machines have been built. They are operating successfully in several German research institutes. This paper deals with basic information on our NPM machines, explains their mode of operation and discusses their performance and efficiency based on an exemplary error analysis.

## 2 Design and operation

An Abbe offset free design (see figure 2) with three miniature interferometers, a user selectable surface-sensing probe and two angular sensors provides extraordinary accuracy [1], [2], [3], [4]. The intersection of all measuring axes of the length measuring systems is the point of contact of the probe with the sample. The measuring object is placed on a moveable mirror corner that is positioned by a three-axis electromagnetic drive system. The position is recorded by three firmly arranged plane mirror interferometers. Translatory errors of the linear guide elements have no influence on the measuring result. Angular errors of the drive system are also measured at the mirror corner by means of optical sensors and used for angular control. Guide error compensation of the linear stages is achieved by a closed loop control system. The data acquisition and control system uses a digital signal processor and specific signal conversion electronics. The possibility to apply different appropriate surface-

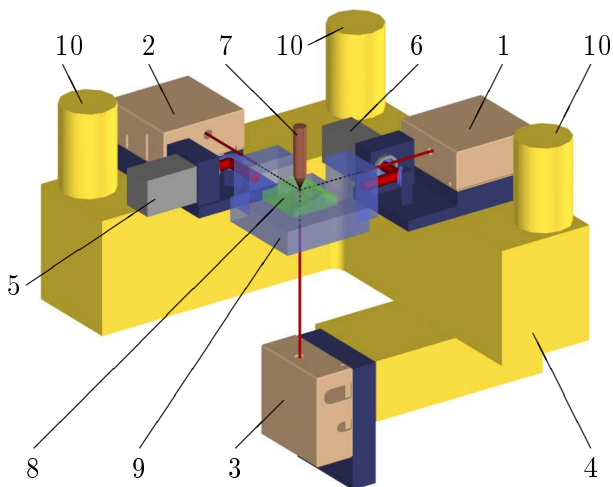


Figure 2: Principle design of the nanomeasuring machine: 1 x-interferometer, 2 y-interferometer, 3 z-interferometer, 4 metrology frame made by Zerodur, 5 roll and yaw angular sensor, 6 pitch and yaw angular sensor, 7 surface-sensing probe, 8 sample, 9 mirror corner, 10 fixing points for probe system

sensing probes allows a wide spectrum of applications. By the use of AFM or STM probes, long range scanning probe microscopy becomes possible.

### 3 Performance and uncertainty

The small uncertainty is achieved by a design following the Abbe comparator principle in combination with the accurate reference coordinate system defined by the mirror corner. Traceability to the national length standard is possible as interferometers based on stabilized HeNe-lasers serve as length measurement systems. The uncertainty of length measurements performed by the NPM machines depends on various uncertainty components [1]. Contributing components are:

- wavelength of frequency stabilized HeNe-Lasers,
- offset, amplitude and phase uncertainty of analog interference signals,
- quantization and rounding errors during the demodulation of interference signals,
- uncertainty of reference coordinate system of the mirror corner,
- uncertainty by calculated refractive index of air,
- thermal expansion of metrology frame, interferometers and probe system and
- uncertainty of length by angular errors (Abbe offset and cosine errors).

The mirror corner of our NPM machine is moved by combination of electromagnetic drives and linear guides in all three linear axes. While there is one drive for each x- and y-axis there are four drives for the z-axis. Therefore the angular errors  $\varphi_x$  and  $\varphi_y$  can be compensated. Looking at one of the three interferometers (figure 3), just two of the three angular errors have an influence on the measuring result as the rotation around the measuring axis is

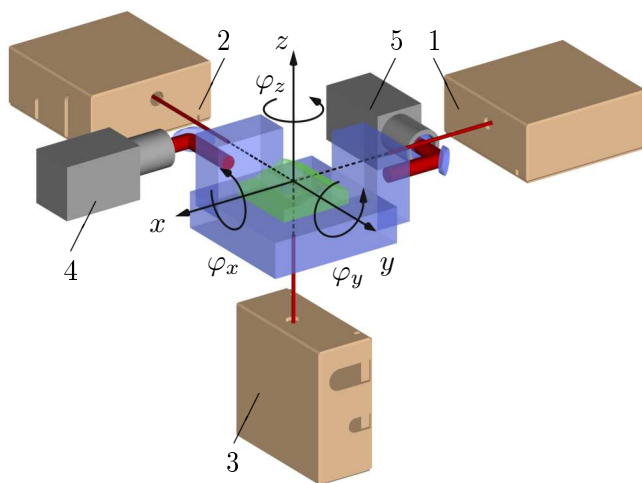


Figure 3: Axes and angle definition of the nanomeasuring machine: 1 x-interferometer, 2 y-interferometer, 3 z-interferometer, 4 roll and yaw angular sensor, 5 pitch and yaw angular sensor

without consequence. For instance, the measuring result of the x-interferometer depends on the rotations  $\varphi_y$  and  $\varphi_z$  where only  $\varphi_y$  can be compensated.

As the interferometers have only one measuring beam with a small diameter, the alignment of the measuring axes on one point can be done with a tilted circular aperture and an optical power meter. This results in residual Abbe offsets of less than 0.1 mm.

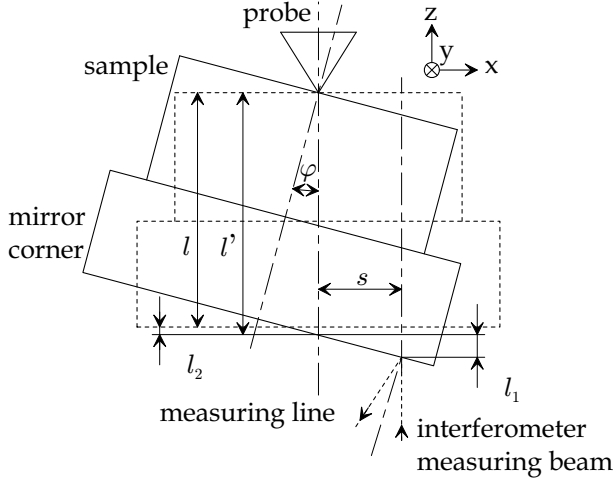


Figure 4: Abbe offset and cosine errors

Figure 4 shows the Abbe offset  $s$ , the Abbe offset error  $\Delta l_1$  and the cosine error  $\Delta l_2$  exemplarily for the z-axis. The angular control systems cause angular uncertainties of x- and y-axis  $u(\varphi_x) = u(\varphi_y) = 0.05''$ , while the rotatory guide errors of the z-axis  $u(\varphi_z) = 5.2''$ . Resulting measurement uncertainties are shown for the x-axis exemplarily in equations 1 to 4. The cosine error depends on displacement  $l_x$  and constructional offset  $l_{x0}$ .

$$u_{1.Ord1}(l_x) = s \cdot \tan(u(\varphi_y)) = 0,03 \text{ nm} \quad (1)$$

$$u_{1.Ord2}(l_x) = s \cdot \tan(u(\varphi_z)) = 1,46 \text{ nm} \quad (2)$$

$$u_{2.Ord1}(l_x) = (l_{x0} - l_x) \cdot \left( \frac{1}{\cos(u(\varphi_y))} - 1 \right) \leq 2,06 \cdot 10^{-6} \text{ nm} \quad (3)$$

$$u_{2.Ord2}(l_x) = (l_{x0} - l_x) \cdot \left( \frac{1}{\cos(u(\varphi_z))} - 1 \right) \leq 7,4 \cdot 10^{-3} \text{ nm} \quad (4)$$

A second type of uncertainty is caused by measurement beam deflection as shown in figure 5. Optical interference signals are converted into electrical signals after passing through a circular aperture. Only axial parts of measurement and reference wavefronts will pass this aperture. Thus a length shortened by  $\Delta l_{geo}$  is measured, resulting in an error  $\Delta l$ .

$$\Delta l_{geo} = a \cdot (\cos(2 \cdot \varphi) - 1) \quad (5)$$

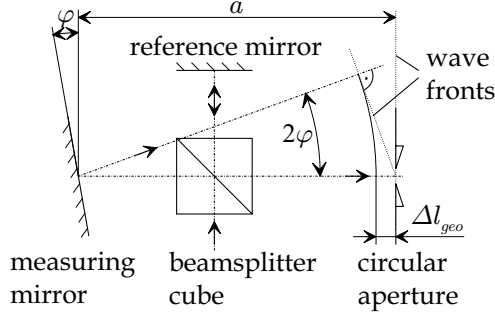


Figure 5: Cosine error of the interferometer

$$\Delta l = \frac{\Delta l_{geo}}{2} = \frac{a \cdot (\cos(2 \cdot \varphi) - 1)}{2} \quad (6)$$

With the angular uncertainties and the system measurement lengths the following uncertainties can be calculated.

$$u_{Int1}(l_x) = \left| \frac{(l_{x1} + l_x)}{2} \cdot (\cos(2 \cdot u(\varphi_y)) - 1) \right| \leq 6,2 \cdot 10^{-6} \text{ nm} \quad (7)$$

$$u_{Int2}(l_x) = \left| \frac{(l_{x1} + l_x)}{2} \cdot (\cos(2 \cdot u(\varphi_z)) - 1) \right| \leq 2,3 \cdot 10^{-2} \text{ nm} \quad (8)$$

The third type of uncertainty to be discussed here is caused by the measuring mirror surface topography. It contributes to the total measurement uncertainty in the way of a cosine error with an angular uncertainty  $u(\varphi_s) = 1.3''$  and leads to the contribution calculated in equation 9.

$$u_{Int3}(l_x) = \left| \frac{(l_{x1} + l_x)}{2} \cdot (\cos(2 \cdot u(\varphi_s)) - 1) \right| \leq 4,0 \cdot 10^{-3} \text{ nm} \quad (9)$$

The discussed uncertainties referred to the x-axis. Uncertainties can be calculated for the y- and z-axis as well. When summed up according to their respective dependencies according to equation 10, they result in the combined uncertainties shown in table 1.

$$\begin{aligned} u^2(l_x) &= (u_{1.Ord1}(l_x) + u_{2.Ord1}(l_x) + u_{Int1}(l_x))^2 \\ &\quad + (u_{1.Ord2}(l_x) + u_{2.Ord2}(l_x) + u_{Int2}(l_x))^2 \\ &\quad + 2 \cdot (u_{Int3}(l_x))^2 \end{aligned} \quad (10)$$

With its design according to the Abbe comparator principle and its angular control systems, the NPM machine shows an extraordinary accuracy.

As thermal expansion has the largest influence on uncertainty, the design of the interferometers is currently revised. The new design uses material with a smaller thermal expansion coefficient for certain parts of the interferometers and adapts their reference beam length to the NPM machine needs. These changes also reduce the contribution of the uncertainty of

	x- and y-axis	z-axis
Minimum	$u(l_{xy}) = 1.48 \text{ nm}$ for $l_x = l_y = 0$	$u(l_z) = 0.035 \text{ nm}$ for $l_z = 0$
Maximum	$u(l_{xy}) = 1.49 \text{ nm}$ for $l_x = l_y = 25 \text{ mm}$	$u(l_z) = 0.036 \text{ nm}$ for $l_z = 5 \text{ mm}$

Table 1: Uncertainties of length by angular errors ( $k_{0,6827} = 1$ )

the calculated index of refraction of air and thus the wavelength of the laser light. Another improvement of the machines has been achieved in the last year by replacing the electrical interferometer signal demodulation modules. The new version features reduced quantization and rounding errors below 0.1 nm. By future implementation of a real-time elliptical regression based on direct signal measurement, the modules will allow fast and accurate correction for nonlinearities caused by offset, amplitude and phase errors of the analog interference signals as well. Our improved NPM machines will have an estimated combined uncertainty of less than 10 nm.

## 4 Acknowledgements

The development of the nanopositioning and nanomeasuring machine is supported by the Thuringian Ministry of Science, Research and Arts. The authors wish to thank all those colleagues who have contributed to the developments described.

## References

- [1] Tino Hausotte. *Nanopositionier- und Nanomessmaschine*. PhD thesis, Technische Universität Ilmenau, 2002.
- [2] G. Jäger, E. Manske, T. Hausotte, and H.-J. Büchner. Laserinterferometrische Nanomeßmaschinen. In *VDI Berichte Nr. 1530 Sensoren und Meßsysteme 2000*, pages 271–278. VDI/VDE-Gesellschaft Meß- und Automatisierungstechnik, März 2000.
- [3] G. Jäger, E. Manske, T. Hausotte, and H.-J. Büchner. Nanomeßmaschinen zur abbe-fehlerfreien Koordinatenmessung. *Technisches Messen*, 67(7-8):319–323, Juli/August 2000.
- [4] G. Jäger, E. Manske, T. Hausotte, H.-J. Büchner, R. Grünwald, and W. Schott. Nanomeasuring technology - nanomeasuring machine. In *The Sixteenth Annual Meeting*, pages 23–27, Crystal City, Arlington, Virginia, 10.-15. November 2001. American Society for Precision Engineering.